

# Numerical Simulation and Experimental Set-up for Predicting the Drying Behavior of Calcium Aluminate Cement (CAC)-Bonded Refractory Castables



M. H. Moreira, A. P. Luz, T. M. Cunha, H. Lemaistre, J. M. Auvray, Chr. Parr, R. Ausas, V. C. Pandolfelli

During the initial heating of Calcium Aluminate Cement (CAC)-bonded castables, physical and chemically-bonded water is released. Therefore, when the refractory's permeability level is limited, pressure buildup inside the dense microstructure can take place, resulting in cracks and spalling of the ceramic lining. Recently, complex models have been developed for the prediction of the temperature, pressure, moisture and displacement fields within dense material. Some of them also consider numerous parameters (i.e., multiple phases, the thermomechanical features and the likely induced damage, etc.), but all rely on complex experiments that depend on multiple thermocouples and pressure transducers. According to these advances, by a joint effort between the university and the CAC binder producer, the present work aims to develop an accessible model based on few parameters, which could be validated and adjusted by simple thermogravimetric experiments. The results pointed out that such a framework is promising and able to satisfactorily predict the overall behavior of the castables' compositions during drying tests. Additionally, the proposed model could also be further validated with current experimental techniques in order to successfully be scaled up and estimate the drying behavior of larger specimens as well as products with more complex geometries.

## 1 Introduction

The initial heat-up of a refractory equipment is always a critical stage, whether it is after its lining or a maintenance procedure. It extends the idle time when the production is on halt and if not properly carried out it can be the main reason for reducing the working life of the ceramic lining.

Additionally, the initial heating of (CAC)-bonded castables is a relevant step because the pressure buildup (due to evaporation of the physical and chemically-bonded water inside the porous matrix) can exceed the

material's mechanical strength, leading to its spalling.

Thus, it is usual to apply very conservative heating up curves of equipment lined with dense ceramic, which can limit their overall productivity and increase the greenhouse gases emission, as they are based on empirical procedures related to the thickness of the material and without considering its geometry or the boundary conditions.

Therefore, numerical models that can predict the heat and mass flux inside the dense castable structure can be of great impor-

tance to estimate the level of triaxial tension produced by the pressure buildup, the effect of the size and the geometry of the ceramic lining, as well as the most suitable boundary conditions to simulate the real scenario commonly attained in the operation of high temperature process.

Most of these mathematical models used for this purpose were developed considering Luikov's equations [1]. Bažant et al. [2] proposed a simplified version of such equations solving them by finite element method to model the behavior of Portland cement-containing concrete at high tem-

M. H. Moreira, A. P. Luz, T. M. Cunha,  
V. C. Pandolfelli  
Federal University of São Carlos (UFSCar),  
Materials Engineering Department  
São Carlos, SP, 13565-905  
Brazil

H. Lemaistre, J. M. Auvray, Chr. Parr  
Imerys  
38090 Vaulx-Milieu, France

R. Ausas  
Institute of Mathematical and Computer  
Sciences (ICMC - USP)  
São Carlos, SP 13566-590  
Brazil

Corresponding author: M.H. Moreira  
E-mail: [moreira.murilo@gmail.com](mailto:moreira.murilo@gmail.com)

Keywords: numerical simulation, castables,  
drying behaviour

Received: 13.07.2019

Accepted: 23.07.2019

peratures, for lining nuclear reactor walls [2]. These authors also assumed that the overall moisture flux was controlled by the flow of adsorbed water through nanopores, thus considering the mass balance equation of the moisture content, regardless the phase of the water inside the porous material.

Afterwards, Gong, et al. [3–5] adapted the previous model for simulating the drying of refractory castable, where a qualitative sensitivity analysis, the influence of impermeable walls and the comparison of different heat-up curves were reported.

Following, Tenchev, et al. [6] considered the multiphase flux of the water content, splitting the mass balance equation into three distinct ones: the first for the air mixture inside the porous, the second for the liquid water and the third for the water vapor. Gawin also considered the mechanical response due to the pressure buildup, developing a thermohygro-mechanical model capable of simulating the damage of the dense structure associated with both, the vapor pressure and thermal spalling [7].

Fey, et al. [8] also developed a multiphase model and calibrated the material parameters used in the simulations with the experimental results obtained for the pressure and temperature of a one-side heated sample. Such experiment is a common method used for assessing the behavior of concrete during its drying. However, the presence of pressure sensors inside the samples may increase the local permeability (due to the thermal expansion mismatch) providing channels for the vapor release [8].

More recently, the nuclear magnetic resonance [9] and neutron tomography [10], which can directly measure the water content distribution inside the humid microstructure, were used to analyze the water release from such materials.

The evolution of the numerical models came with the expense of increased complexity without any clear improvement on its accuracy, demanding fitting of parameters to adjust the experimental results. These evidences support Bažant’s statement that the multiphase flow increases the complexity introducing errors due to the assessment of other properties required for such simulations [11].

Therefore, the purpose of the present work is to apply a simplified model, based on

Bažant’s assumptions, and data collected from thermogravimetric experiments to validate this single-phase calculation and predict the drying behavior of refractory castables.

## 2. Materials and Method

### 2.1. Numerical Model

Considering Bažant’s [2] model and using the temperature,  $T$  [°C], and pore pressure,  $P$  [Pa] as the independent variables, one can define the mass and energy conservation eq. (1) and (2):

$$\underbrace{\frac{\partial w}{\partial t}}_{(a)} = \underbrace{\nabla \cdot \left( \frac{K}{g} \nabla P \right)}_{(b)} + \underbrace{\frac{\partial w_d}{\partial t}}_{(c)} \quad (1)$$

$$\underbrace{\rho C_p \frac{\partial T}{\partial t}}_{(a)} = \underbrace{C_a \frac{\partial w}{\partial t}}_{(b)} + \underbrace{C_w \frac{K}{g} \nabla P \cdot \nabla T + \nabla \cdot (\lambda \nabla T)}_{(d)} \quad (2)$$

where, the first term on the left hand side of eq. (1), (a), is the variation in time, [s], of the free evaporable water per cubic meter of concrete,  $w$  [kg · m<sup>-3</sup>], which due to mass conservation is equivalent to (b) plus (c), which describes the flux of moisture following Darcy’s law (where  $K$  and  $g$  are defined in eq. 3) and the time rate of dehydration water release by cubic meter of concrete [kg · m<sup>-3</sup>], respectively.

Eq. (2) is comprised by term (a) which considers the variation of thermal energy (where  $\rho$  is the density and  $C_p$  the specific heat) with time, and must be equal to the

evaporation heat (where  $C_a$  is the evaporation heat of water [J · kg<sup>-1</sup>]), (b), the convective transport of heat (where  $C_w$  is the specific heat of water [J · kg<sup>-1</sup> · K<sup>-1</sup>]), (c), and the heat conducted through the concrete (where  $\lambda$  is its thermal conductivity), (d).

The free evaporable water is considered equivalent to the sorption isotherms, which are functions of the temperature,  $T$  [°C] and the relative humidity,  $\Phi$  [–]. Thus, their derivatives with respect to time can be calculated by the partial derivatives of the independent variables of the problem,  $T$  and  $P$ . The partial derivatives of  $w$  are calculated by the central finite difference method. The sorption isotherms are defined by semi-empirical relations proposed by Bažant, et al. [2] and adjusted by Gong, et al. [3], which were used by the present authors for the refractory castable described in Tab. 1.

The simulation of the castable behavior during the thermogravimetric analysis (TGA) was carried out by a 3D-mesh with 33920 elements and a time step of 30 s. The boundary conditions used were the mass convection and the radiation heating (with a source temperature equal to the furnace heating rate) on the sides of the sample as shown in Fig. 1.

### 2.2 Experimental measurements

A dense CAC-bonded refractory castable was prepared as a reference material (Tab. 1) in order to obtain the parameters needed for the model.

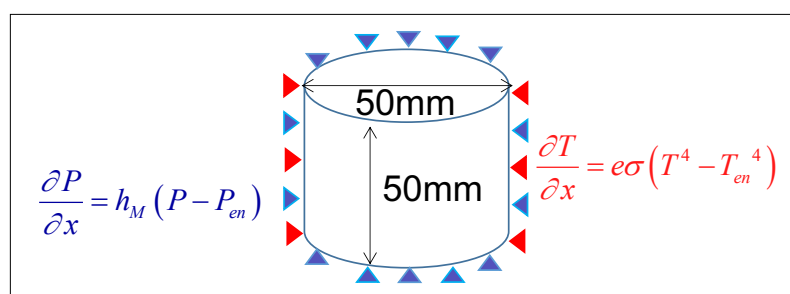


Fig. 1 Numerical setup of the TGA test

Tab. 1 Reference composition characterized and tested on the TGA experiment

Raw Material	Composition [mass-%]
Tabular Alumina (AT, d < 6 mm)	74
Calcined alumina (CL370)	11
Reactive alumina (CT3000SG)	10
Calcium aluminate cement (Secar 71)	5
Distilled water	4,5

The apparent density  $\rho$  [kg · m<sup>-3</sup>] of the samples cured at 30 °C, dried at 110 °C and fired at 150 °C, 200 °C, 250 °C and 350 °C for 5 h was measured by the Archimedes principle, using kerosene as the immersion liquid. The hot parallel wire technique (Netzsch TCT 426) was carried out according to ISO 8894-2 to measure the thermal conductivity  $\lambda$  [W · m<sup>-1</sup> · K<sup>-1</sup>] of brick samples and to calculate the heat capacity of such materials  $C_p$  [J · kg<sup>-1</sup> · K<sup>-1</sup>].

The intrinsic permeability was measured following ASTM C577 standard at room temperature (RT) and using samples previously dried at 110 °C, and fired at 150 °C, 200 °C, 250 °C and 350 °C for 5 h.

The model uses the intrinsic permeability,  $K$  [m · s<sup>-1</sup>], defined by eq. (3), whereas the equipment measures the Forchheimer coefficients  $k_1$  [m<sup>2</sup>] and  $k_2$  [m · s<sup>-1</sup>] [12].

$$\frac{K}{g} = \frac{k_1 \rho_{air}}{\mu_{air}} \quad (3)$$

where,  $g$  is the gravity acceleration [m · s<sup>-2</sup>],  $\rho_{air}$  [kg · m<sup>-3</sup>] is the air density at RT, and  $\mu_{air}$  is the dynamic viscosity of air at RT [Pa · s]. Tab. 2 summarizes the properties used for the model.

The thermogravimetric analysis of the castable was carried out in a furnace equipped with two thermocouples (one for monitoring the furnace temperature and another for the sample's one) and a scale with a digital acquisition system. Thus, it was possible to record the mass loss of the samples as a function of temperature and, by differentiating such curve, their mass loss rate (DTG) could be obtained. The experimental TGA test was performed with a con-

Tab. 2 Properties used on the model

Properties	Values
Thermal conductivity*, $\lambda$ [W · m <sup>-1</sup> · K <sup>-1</sup> ]	11,5 – 0,029*T + 3,88*T <sup>2</sup> – 1,89*T <sup>3</sup>
Density*, $\rho$ [kg/m <sup>3</sup> ]	3219 – 0,44*T + 0,00027*T <sup>2</sup>
Permeability*, $K$ [m · s <sup>-1</sup> ]	11,5 – 0,29*T + 3,88*T <sup>2</sup> – 1,89*T <sup>3</sup>
Specific heat, $C_p$ [J · kg <sup>-1</sup> · K <sup>-1</sup> ]	730
Specific heat of water, $C_w$ [J · kg <sup>-1</sup> · K <sup>-1</sup> ]	4100
Estimated emissivity, $e$ [–]	0,9
Mass transfer coefficient, $h_m$ [s · m <sup>-1</sup> ]	1 x 10 <sup>-4</sup>
Ambient vapor pressure, $P_{en}$ [Pa]	2850
Amount of cement per kg of castable, $w_c$ [kg · m <sup>-3</sup> ]	153,34
Saturation water content at RT per kg of castable, $w_0$ [kg · m <sup>-3</sup> ]	40

\*Values interpolated in the range [25 °C, 600 °C]

stant heating rate of 2 °C/min, 5 °C/min or 20 °C/min using cylindrical samples with 50 mm of diameter and 50 mm of height, after curing at 30 °C for 24 h or drying at 110 °C for obtaining wd.

### 3 Results and discussion

The fields of  $P$  and  $T$  inside the castable sample can be calculated by solving eq. (1) and (2) and using the data presented in Tab. 2. Fig. 2 shows the results obtained for the surface temperature of the samples (which may be compared to the temperature value obtained experimentally by the thermocouple), the evolution of the maximum pressure inside the material (which can be compared to the Antoine's pressure) and the  $P$  distribution in a cylindrical sample at the end of the TGA carried out with a 5 °C/min heating rate.

The simulations resulted in lower heating rate until the end of physically adsorbed water (the pronounced peak close 60 min

for the 5 °C/min and 120 min for the 2 °C/min) when compared with the experimental data. Afterwards, the calculated heating rate was higher than the experimental one. Such results may indicate that the present measurements of the dehydration water ( $w_d$ ) and the use of Bažant's sorption isotherms ( $w$ ) were not properly representing the kinetics of the phase transformations of the system.

When considering the pressure evolution, the only sample that exploded (heated at a rate of 20 °C/min) was the one with a higher peak of pore pressure, which agrees with the modelling results, especially when analyzing the pressure profile that concentrates the highest values in the middle of the sample.

In order to compare the mass release provided by the numerical model with the experimental results, the amount of evaporable water and the dehydration one were integrated over the domain volume.

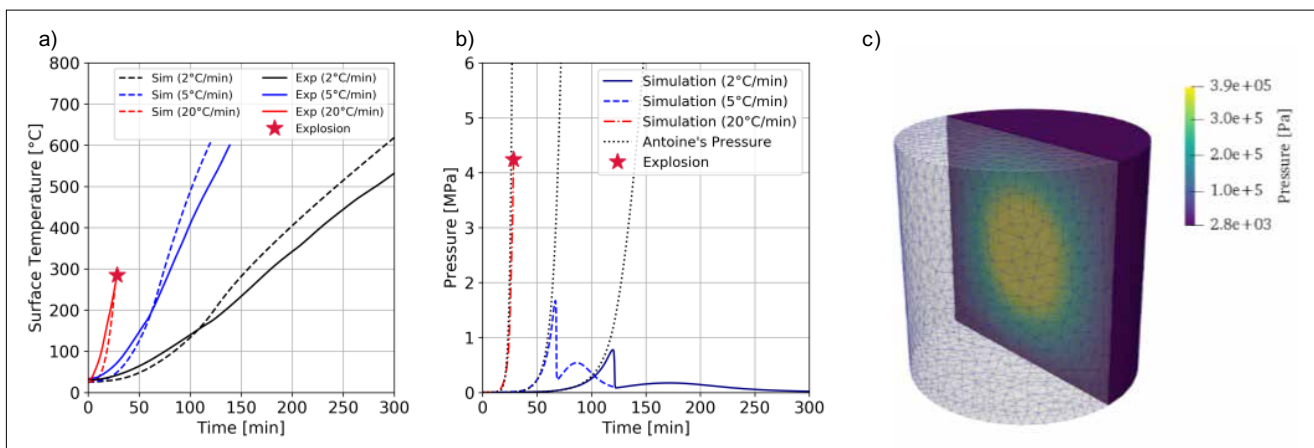
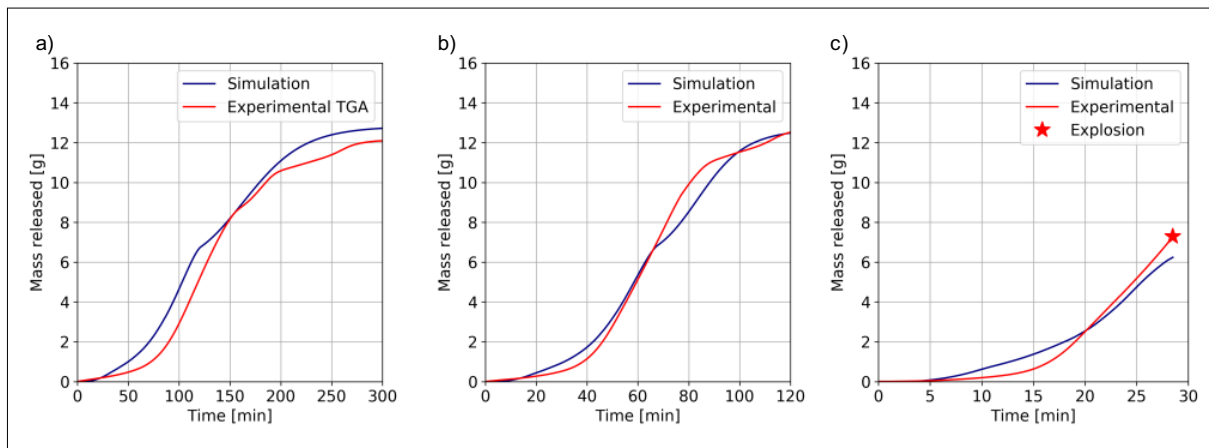


Fig. 2 (a) Surface temperature evolution ("Sim" refers to simulation, and "Exp" to experimental), (b) maximum pressure evolution, and (c) final pressure distribution of the sample heated at a 5 °C/min rate



**Fig. 3** Comparison of experimental (red filled curves), and numerical (dark blue dashed curves) mass release for heating rates of 2 °C/min (a), 5 °C/min (b), and 10 °C/min (c). Inset c) shows the results using an adjusted  $w_d$

Fig. 3 presents the numerical and experimental results for 3 distinct heating rates, 2 °C/min (a), 5 °C/min (b), and 10 °C/min (c). There is a fair agreement among them for the initial moments of heating, where most of the water release is due the evaporable water. At high temperatures (longer times), an increasing discrepancy of the results is observed.

This might be related to the methodology used to obtain the dehydration curve,  $w_d$ , which was evaluated by a TGA test with samples previously dried at 110 °C for 24 h, contrary to the validation tests which were carried out after curing at 30 °C for 24 h. This may lead to the formation of distinct phases in the castable structure, which may not be formed during drying of cured samples analyzed on the TGA experiment. Such phases would be decomposed at higher temperatures as shown by the use of an adjusted  $w_d$  (Fig. 3c), which results in a better agreement. Another possible explanation for the lack of accuracy may be due to the use of an inappropriate set of sorption isotherms.

#### 4 Conclusions

The present work describes both, a simplified model and a usual experimental setup that can be used for the optimization of heating up curves of (CAC)-bounded compositions.

The single-phase model based on Bažant's work was able to qualitatively represent the behavior of the TGA curves measured

experimentally. Such approach could be also applied to model complex geometries and multiple boundary conditions of components used in industrial cases, after a validation with a pressure, temperature and moisture test (PTM).

In order to improve the accuracy of the model, better experimental measurements of key properties may be needed such as, a direct measure of the sorption isotherms, drying of the samples used on the dehydration tests at lower temperatures (i.e. controlling the relative humidity) and a methodology to estimate  $h_m$ .

Nonetheless, the model developed herein displays analogous results to multiphase models, but with the advantage of depending on less variables (only 6 material properties vs. 14 needed for the multiphase models) and on a simpler experimental setup.

#### Acknowledgements

The authors are greatly thankful for the FIRE support and Imerys for sponsoring this work; Almatix for supplying the calcined aluminas, and Dr Christoph Wohrmeyer (Imerys) for discussions.

#### References

- [1] Alexei Luikov (Ed.): Heat and mass transfer in capillary-porous bodies. Oxford 1966, 3–10
- [2] Bažant, Z.P.; Thonguthai, W.: Pore pressure in heated concrete walls: Theoretical prediction. Mag. Concr. Res. **31** (1979) [107] 67–76

- [3] Gong, Z.X.; Mujumdar, A.S.: The influence of an impermeable surface on pore pressure during drying of refractory concrete slabs. Int. J. Heat Mass Transf. **38** (1995) [7] 1297–1303
- [4] Gong, Z.X.; Song, B.; Mujumdar, A.S.: Numerical simulation of drying of refractory concrete. Drying Technol. **9** (1991) [2] 479–500
- [5] Gong, Z. X.; Mujumdar, A.S.: A model of kiln-drying for refractory concrete. Drying Technol. **11** (1993) [7]
- [6] Tenchev, R.T.; Li, L.Y.; Purkiss, J.A.: Finite element analysis of coupled heat and moisture transfer in concrete subjected to fire. Numer. Heat Transf. Part A, Appl. **39** (2001) [7] 685–710
- [7] Gawin, D.; Majorana, C.E.; Schrefler, B.A.: Numerical analysis of hygro-thermic behaviour and damage of concrete at high temperature. Mech. Cohesive-frictional Mater. **4** (1999) [1] 37–74
- [8] Fey, K.G.; et al.: Experimental and numerical investigation of the first heat-up of refractory concrete. Int. J. Therm. Sci. **100** (2016) 108–125
- [9] Oummadi, S.; et al.: Distribution of water in ceramic green bodies during drying. J. Europ. Ceram. Soc. **39** (2019) 3164–3172
- [10] Dauti, D.; et al.: Modeling of 3D moisture distribution in heated concrete: from continuum towards mesoscopic approach. Int. J. Heat Mass Transf. **134** (2019) 1137–1152
- [11] Bažant, Z.P.; Jirásek, M.: Creep and hygrothermal effects in concrete structures. Dordrecht 2018, 628–629
- [12] Innocentini, M.D.M.; Pardo, A.R.F.; Pandolfelli, V.C.: Influence of air compressibility on the permeability evaluation of refractory castables. J. Amer. Ceram. Soc. **83** (2000) [6] 1536–1538